FIGURES

Project logo

Figures mentioned in submitted text

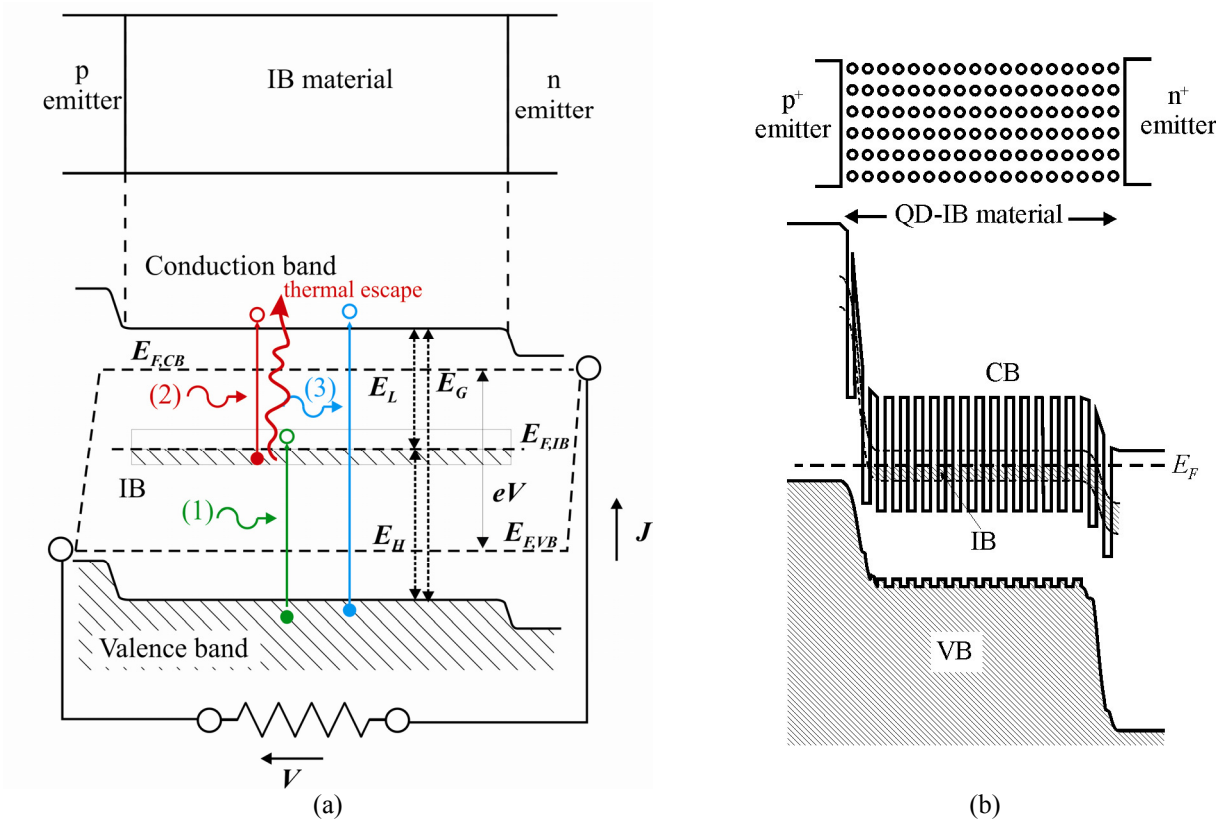

Fig. 1(a) Intermediate band solar cell: layout, photon absorption processes and quasi-Fermi levels. (b) Implementation with quantum dots.

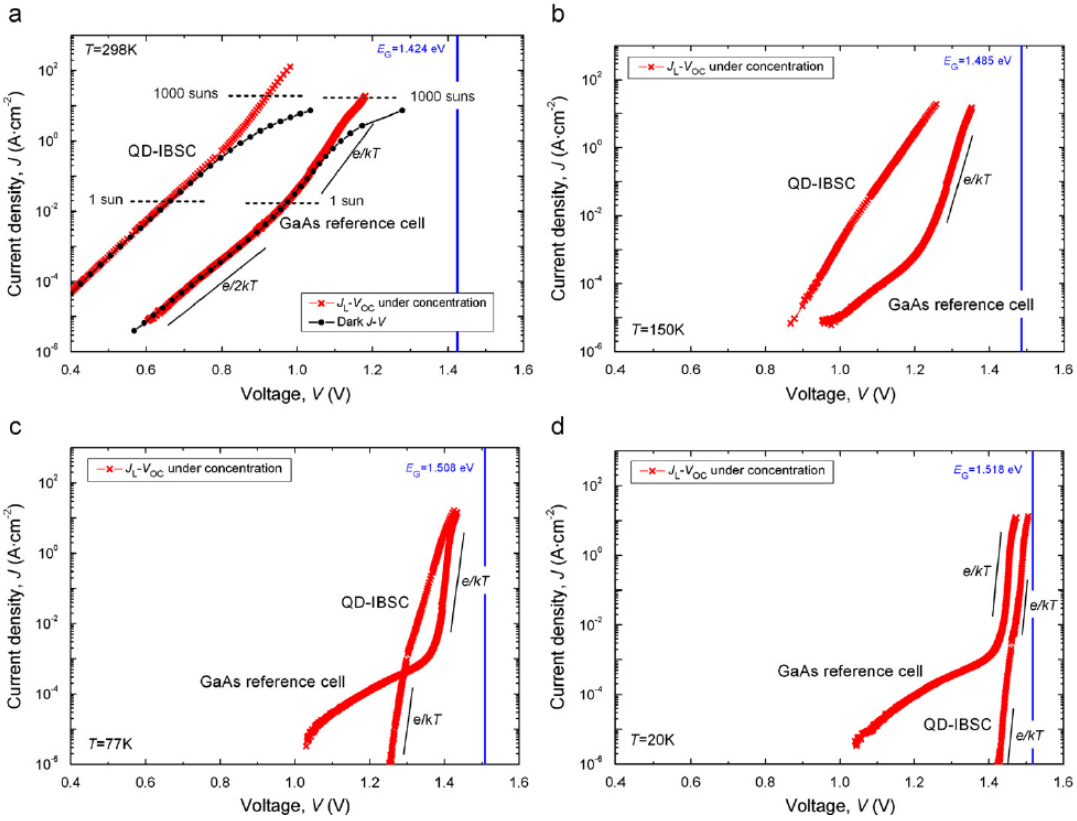

Fig. 2. Concentrated light J_L–V_{OC} characteristics of both the QD-IBSC and the reference cell at different temperatures. (a) Dark J–V and concentrated light J_L–V_{OC} characteristics measured at T=298 K. The concentration levels are indicated with horizontal gray dashed lines. (b), (c) and d) show concentrated light J_L–V_{OC} measurements at T=150 K, T=77 K and T=20 K respectively. The solar cell fundamental bandgap is represented with a solid, blue line for each temperature [Copyright 2011 Elsevier. This figure may be downloaded for personal use only. Any other use requires prior permission of the author and Elseviercs. The figure appeared in [P. G. Linares, A. Martí, E. Antolín, C. D. Farmer, I. Ramiro, C. R. Stanley, and A. Luque, Solar Energy Materials and Solar cells 98, 240-244 (2011).] and may be found at (http://dx.doi.org/10.1016/j.solmat.2011.11.01520)]

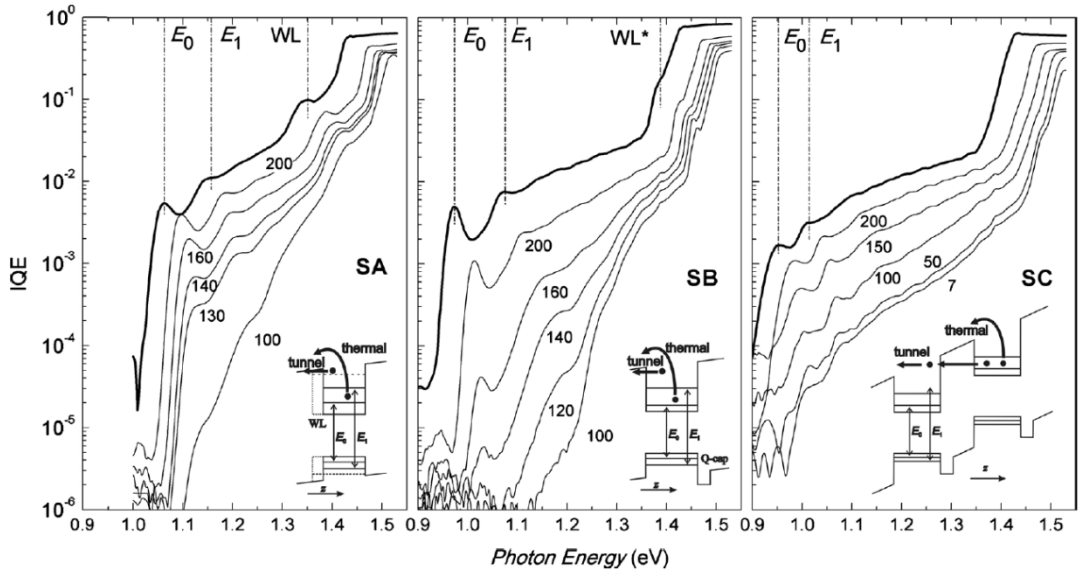

Fig.3. Internal quantum efficiency of different QD-IBSCs. Only in samples SA and SB the below bandgap photocurrent is suppressed indicating they are good candidates for voltage preservation. In sample SC, the sub bandgap photocurrent is not suppressed due to the existence of tunnelling that also causes carriers to escape [Copyright 2010 American Institute of Physics. This figure may be downloaded for personal use only. Any other use requires prior permission of the author and the American Institute of Physics. The figure appeared in [E. Antolin, A. Marti, C. D. Farmer, P. G. Linares, E. Hernandez, A. M. Sanchez, T. Ben, S. I. Molina, C. R. Stanley, and A. Luque, Journal of Applied Physics 108, 064513 (2010)] and may be found at (http://dx.doi.org/10.1063/1.3468520)]

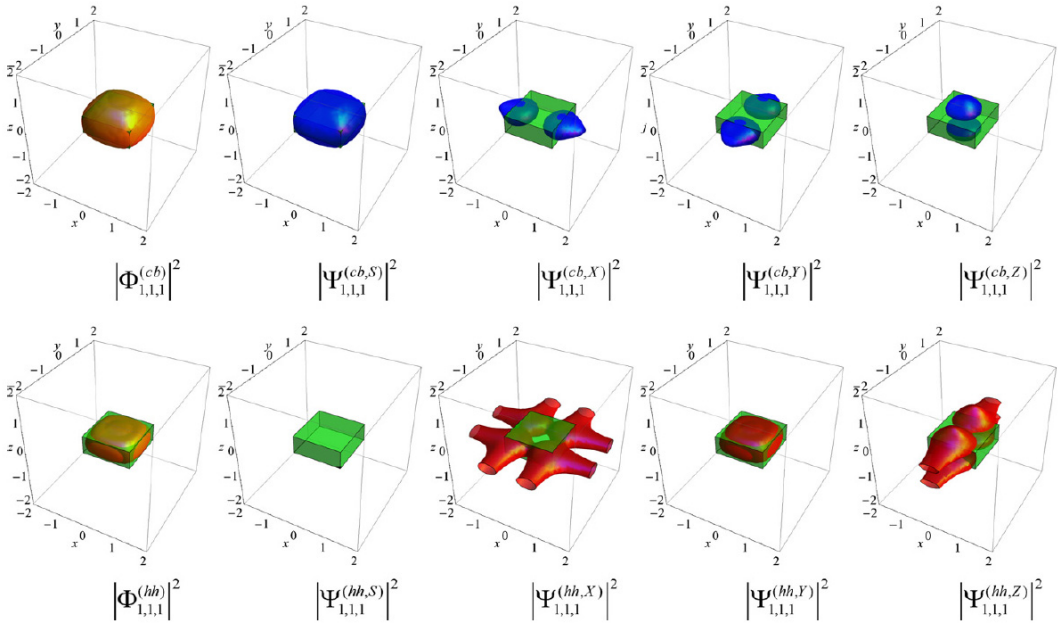

Fig. 4. Contour plots of the wavefunction corresponding to the electrons confined in the quantum dot at different energy levels. [Copyright 2011 Elsevier. This figure may be downloaded for personal use only. Any other use requires prior permission of the author and Elseviercs. The figure appeared in A. Luque, A. Martí, E. Antolín, P. G. Linares, I. Tobías, I. Ramiro, and E. Hernandez, Solar Energy Materials and Solar cells 95, 2095-2101 (2011) and may be found at (doi: 10.1016/j.solmat.2011.02.028)].

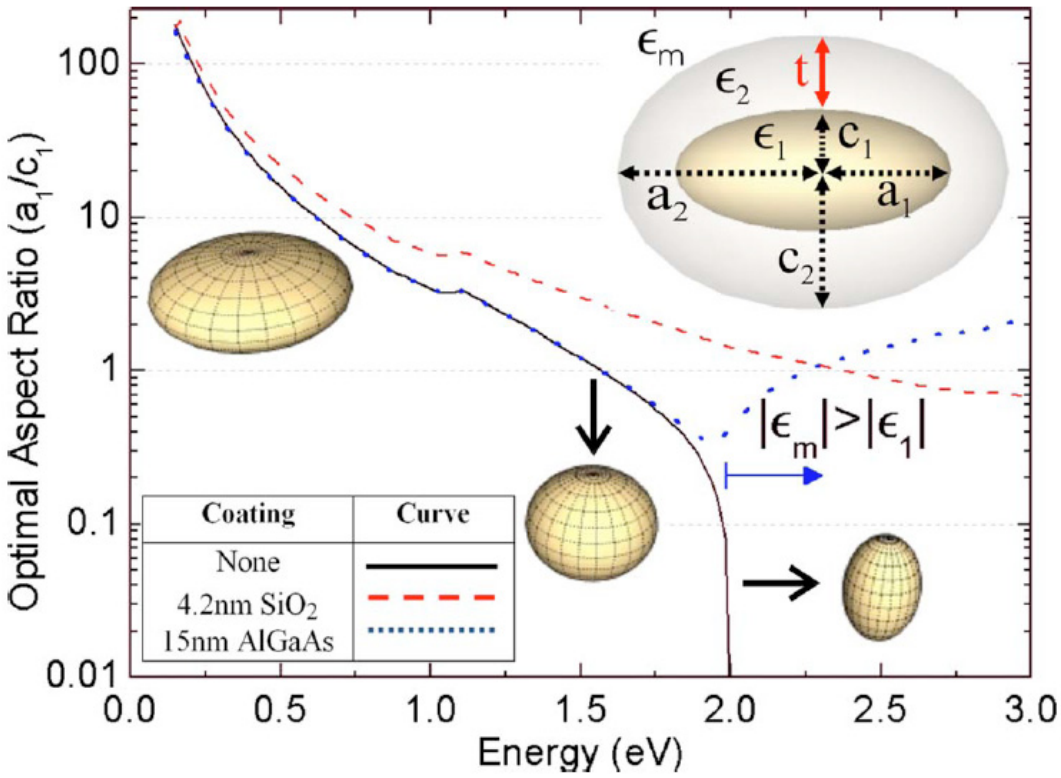

Fig. 5. Spheroid aspect ratios that maximize the polarizability for coated and uncoated Ag metal nanoparticles in GaAs medium. [Copyright 2009 American Institute of Physics. This figure may be downloaded for personal use only. Any other use requires prior permission of the author and the American Institute of Physics. The figure appeared in M. J. Mendes, A. Luque, I. Tobias, and A. Marti, Applied Physics Letters 95, 071105-3 (2009)] and may be found at http://link.aip.org/link/doi/10.1063/1.3205470].

(a)

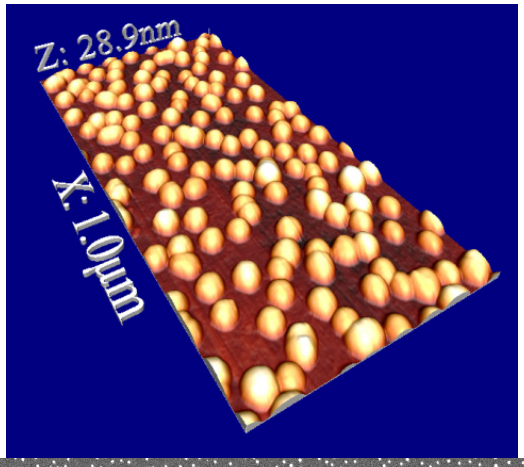

(b)

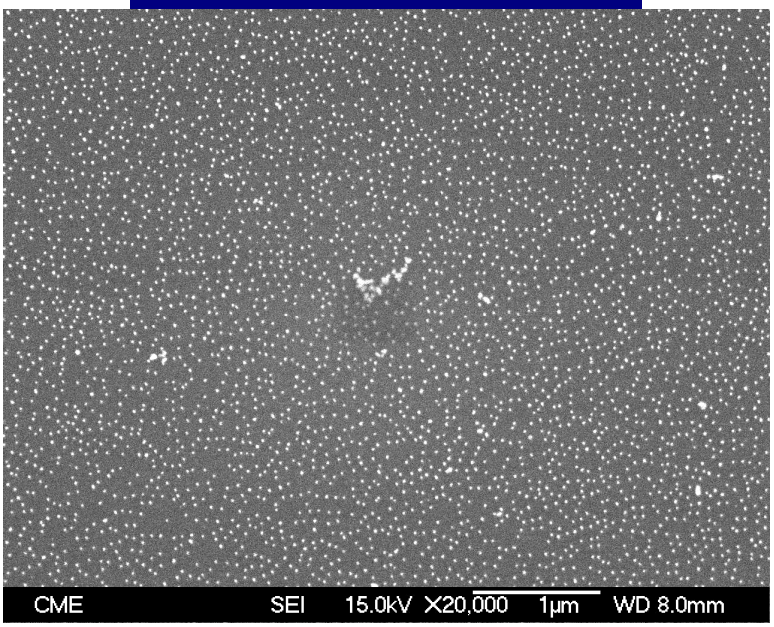

Fig. 6. Essays of deposition of metal nanoparticles on silicon substrates that have taken place during the Poject.

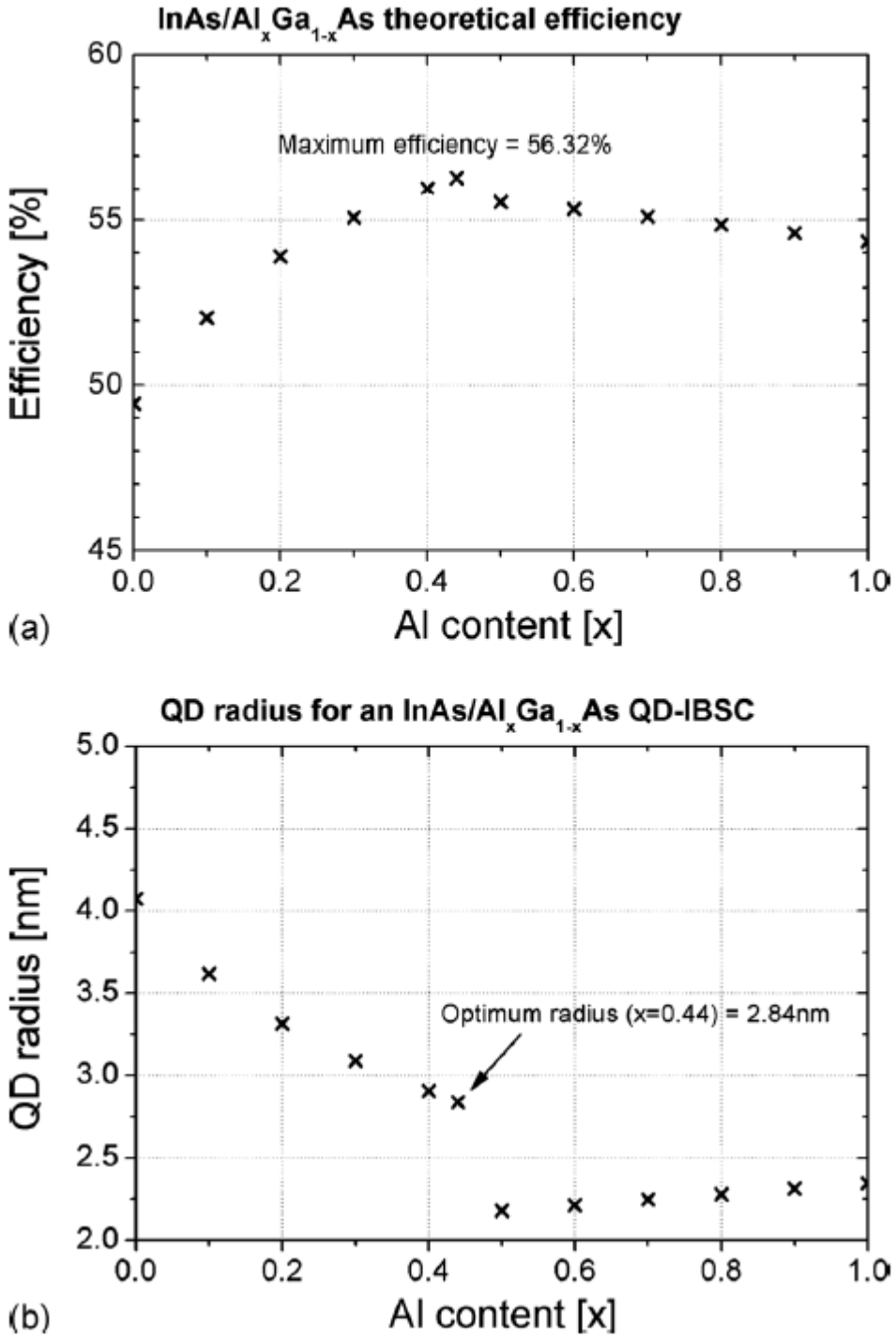

Fig. 7. (a) Theoretical efficiency limit of the InAs/AlxGa1−xAs QD-IBSC in accordance with the Al content and calculated for its optimum radius. (b) Radius of the optimum quantum sphere corresponding to the first excited level appearance in accordance with the Al content. [Copyright 2011 American Institute of Physics. This figure may be downloaded for personal use only. Any other use requires prior permission of the author and the American Institute of Physics. The figure appeared in P. G. Linares, A. Marti, E. Antolin, and A. Luque, Journal of Applied Physics 109, 014313-8 (2011)] and may be found at http://link.aip.org/link/doi/10.1063/1.3527912].

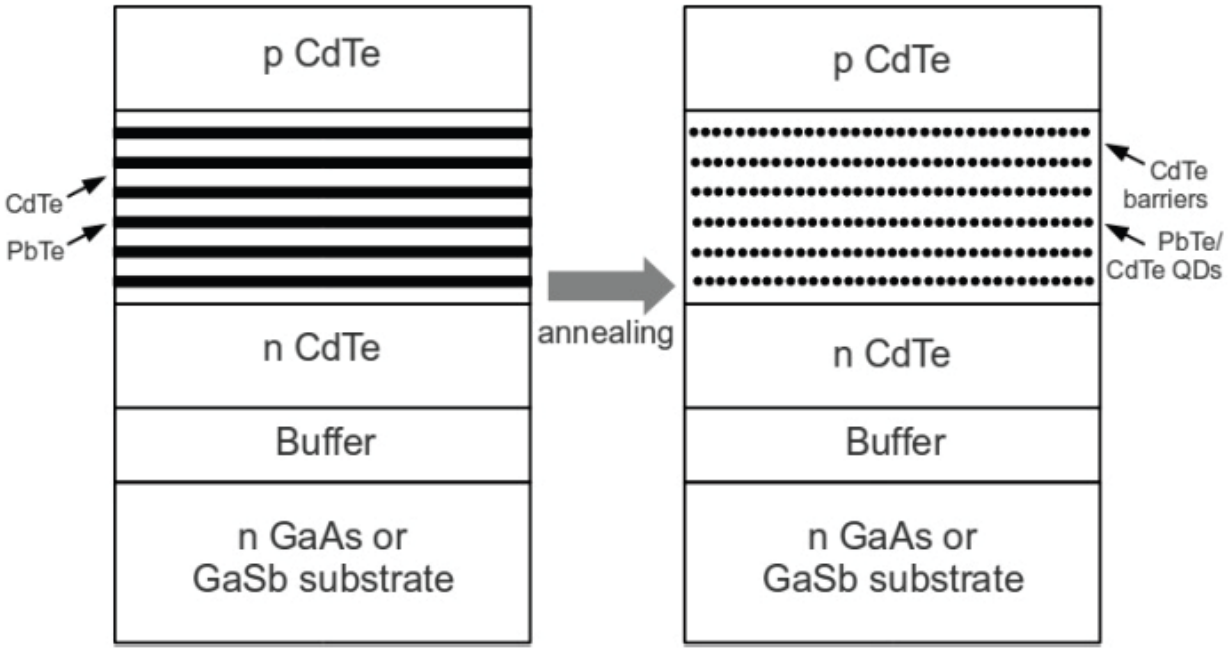

Fig. 8. Example of a lead salt QD-IBSC structure using PbTe/CdTe QDs as IB material, and CdTe p- and n-emitters. [Copyright 2011 IEEE. This figure may be downloaded for personal use only. Any other use requires prior permission of the author and IEEE. The figure appeared in E. Antolín, A. Martí, and A. Luque, Proc. 37th IEEE PVSC (2011).]

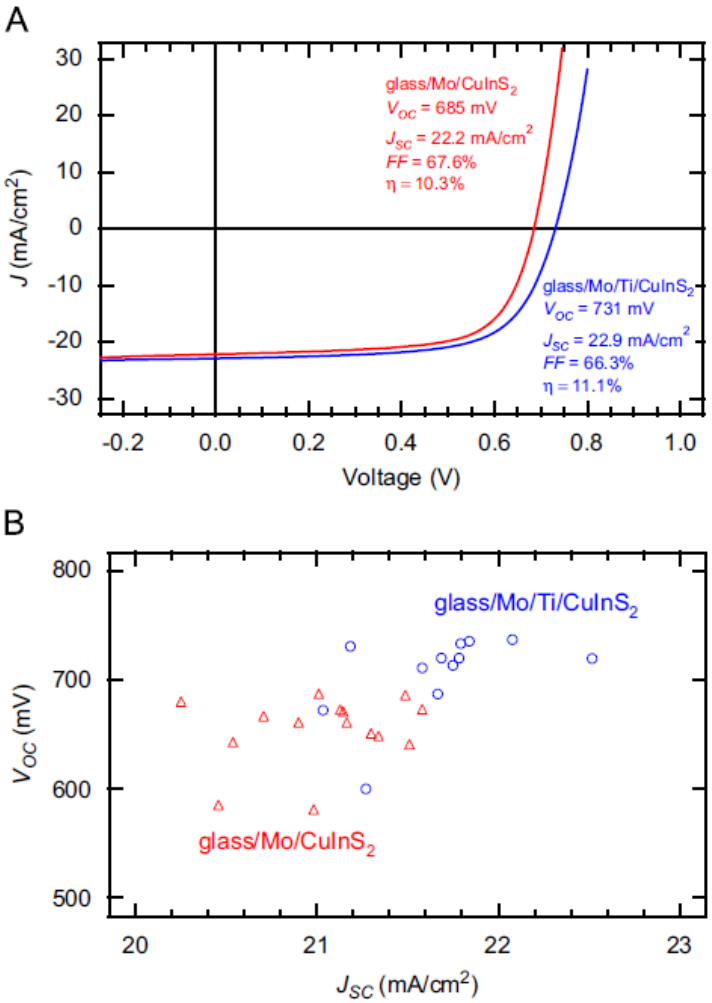

Fig. 9. (A) Current–voltage curves for glass/Mo/CuInS2 and glass/Mo/Ti/CuInS2 solar cells recorded at room temperature under simulated 1-sunAM1.5light,and (B) scatter plot of (roomtemperature,1-sun) open-circuit voltage vs short-circuit current for Ti-containing (circles) and Ti-free CuInS2 solar cells (triangles) from the same absorber process batch. [Copyright 2010 Elsevier. This figure may be downloaded for personal use only. Any other use requires prior permission of the author and Elseviercs. The figure appeared in B. Marsen, L. Steinkopf, I. Lauermann, M. Gorgoi, H. Wilhelm, T. Unold, R. Scheer, and H. W. Schock, Solar Energy Materials and solar Cells, 1730-1733 (2010). and may be found at (doi:10.1016/j.solmat.2010.05.036)]

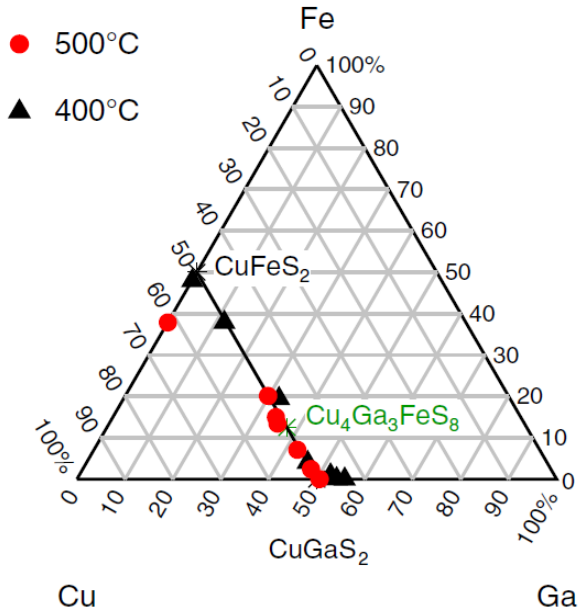

Fig. 10. Ternary diagram showing the relative contents of Cu, Ga and Fe in the Cu–Ga–Fe–S films (after cyanide etch) [Copyright 2011 Elsevier. This figure may be downloaded for personal use only. Any other use requires prior permission of the author and Elsevier. The figure appeared in B. Marsen, S. Klemz, G. Landi, L. Steinkopf, R. Scheer, S. Schorr, and H. W. Schock, Thin Solid Films (2011) and may be found at doi:10.1016/j.tsf.2011.01.137]

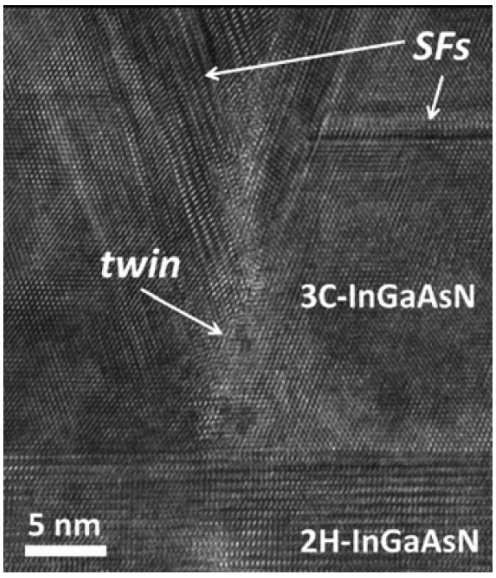

Fig. 11. HRTEM micrograph highlighting planar defects formed after the onset of the hexagonal to cubic InGaAsN transformation. [Copyright 2011 Elsevier. This figure may be downloaded for personal use only. Any other use requires prior permission of the author and Elsevier. The figure appeared in F. M. Morales, D. Carvalho, T. Ben, R. García, S. I. Molina, A. Martí, A. Luque, C. R. Staddon, R. P. Campion, and C. T. Foxon, Scripta Materialia 66, 351-354 (2011)] and may be found at http://dx.doi.org/10.1016/j.scriptamat.2011.11.025]

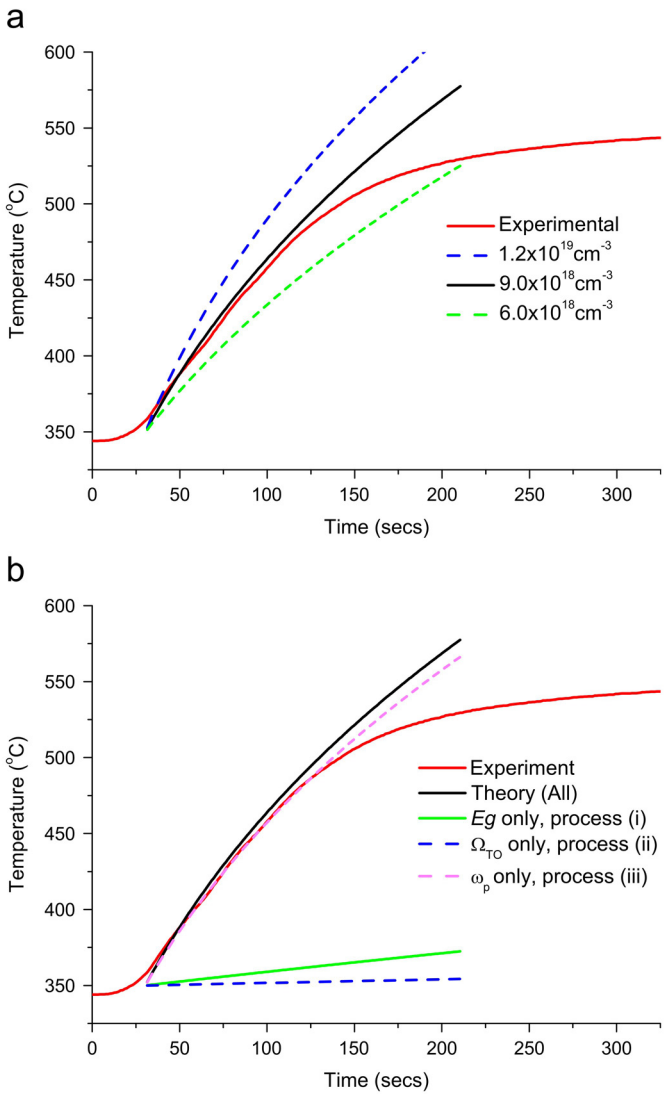

Fig. 12. Experimental and simulated evolution of substrate temperature during growth of InN on GaAs. (a) Shows a range of simulated curves produced using carrier concentration N values of 6E18, 9E18 and 1.2E19 cm-3 (b) Simulated evolution using N=9E18 cm-3 of substrate temperature during growth of InN on GaAs. Also shown is the individual effect of absorption due to bandgap (Eg), freecarriers(ωp) and phonons (ΩTO) only. [Copyright 2010 Elsevier. This figure may be downloaded for personal use only. Any other use requires prior permission of the author and Elsevier. The figure appeared in 1 J. L. Hall, A. J. Kent, C. T. Foxon, and R. P. Campion, Journal of Crystal Growth 312, 2083-2088 (2010) and may be found at doi:10.1016/j.jcrysgro.2010.04.030]